Published in final edited form as:
*Pediatr Blood Cancer*. 2010 July 1; 54(7): 921–926. doi:10.1002/pbc.22367.

# Initial Testing of a Monoclonal Antibody (IMC-A12) against IGF-1R by the Pediatric Preclinical Testing Program

**Peter J. Houghton, PhD**[1], **Christopher L. Morton**[1], **Richard Gorlick, MD**[2], **E. Anders Kolb, MD**[3], **Stephen T. Keir, PhD**[4], **C. Patrick Reynolds, MD, PhD**[5], **Min H. Kang, PharmD**[5], **John M. Maris, MD**[6], **Jianrong Wu**[1], and **Malcolm A. Smith, MD, PhD**[7]

[1] St. Jude Children's Research Hospital, Memphis, TN.

[2] The Children's Hospital at Montefiore, Bronx, NY.

[3] A.I. duPont Hospital for Children, Wilmington, DE.

[4] Duke University Medical Center, Durham, NC.

[5] Texas Tech University Health Sciences Center, Lubbock, TX.

[6] Children's Hospital of Philadelphia, University of Pennsylvania School of Medicine and Abramson Family Cancer Research Institute, Philadelphia, PA.

[7] Cancer Therapy Evaluation Program, NCI, Bethesda, MD.

## Abstract

**Background—**Many childhood malignancies including sarcomas, neuroblastoma and Wilms tumor show the presence of both, active, type-1-insulin-like growth factor receptor (IGF-1R), and the autocrine production of its ligands IGF-1/IGF-2. IMC-A12 is a fully human IgG1 antibody that prevents ligand binding to the IGF-1R.

**Procedures—**IMC-A12 was evaluated against the 23 cell lines of the Pediatric Preclinical Testing Program (PPTP) *in vitro* panel using 96 hour exposure at concentrations ranging from 0.01 nM to 0.1 μM. IMC-A12 was tested *in vivo* at a dose of 1 mg/mouse administered intraperitoneally twice weekly for six weeks.

**Results—***In vitro*, IMC-A12 induced T/C values less than 50% in only three cell lines, a rhabdomyosarcoma cell line (Rh41) and two Ewing sarcoma cell lines (TC-71 and CHLA-9). *In vivo*, IMC-A12 induced significant differences in EFS distribution compared to control in 24 of 34 (71%) evaluable solid tumor xenografts. Using the PPTP "time to event" activity measure, IMC-A12 induced intermediate (n=13) or high (n=1) activity in 33 xenografts evaluable for this activity measure, including 6 of 6 rhabdomyosarcoma xenografts, 3 of 5 osteosarcoma xenografts, 2 of 5 neuroblastoma xenografts, and 1 of 5 Ewing sarcoma xenografts. The only objective response observed was observed in a rhabdomyosarcoma xenograft (Rh28) that achieved a maintained complete response.

**Conclusions—**IMC-A12 demonstrated broad antitumor activity against the PPTP's *in vivo* solid tumor panels, with the activity primarily being tumor growth inhibition rather than tumor regression. IMC-A12 showed its greatest activity *in vivo* against the PPTP's rhabdomyosarcoma xenografts.

Corresponding Author: Peter J. Houghton, PhD Department of Molecular Pharmacology St. Jude Children's Research Hospital 262 Danny Thomas Place Memphis, TN 38105 Voice: (901) 595-3440 Fax: (901) 595-4290 peter.houghton@stjude.org .

**Keywords**

Preclinical Testing; Developmental Therapeutics; IMC-A12

## INTRODUCTION

Many childhood cancers (rhabdomyosarcoma, osteosarcoma, Ewing sarcoma, neuroblastoma, and Wilms tumor) show the presence of both active type-1 insulin-like growth factor receptor (IGF-1R) and the autocrine production of its ligands IGF-1 and or IGF-2 [1]. IGF-1 and −2 and IGF-1R regulate all aspects of the malignant phenotype with IGF-1R being activated by its ligands and also by steroid hormones [2-4]. The activated IGF-IR is capable of phosphorylating other tyrosine-containing substrates of which the insulin receptor substrates (IRS-I-4) link the receptor to a cascade of enzyme activations via PI3K-Akt-mTOR and RAF-MAPK systems [5].

The role of IGF-1R signaling in the pathogenesis of childhood cancer, and its role in preventing apoptosis induced by a multitude of cellular stresses including cytotoxic drugs, radiation and hypoxia [6] indicate that targeting this pathway may have considerable utility for therapy of these rare cancers. As dysregulated IGF-I signaling is common to several adult malignancies, targeting IGF-IR has become a major focus for therapeutic development [6-12]. Currently there are both small molecule drugs and fully human or humanized antibodies directed at the IGF-1R. Five fully human (CP-751,871, AMG 479, R1507, IMC-A12, SCH717454) or humanized antibodies (H7C10/MK0646) are in adult phase-I to −III clinical trials. These agents show specificity for IGF-IR although they may inhibit chimeric receptors formed through heterodimerization with the insulin receptor. In preclinical models of childhood cancers, the prototypical anti-IGF-1R antibody, α-IR3, was shown to mediate down regulation of IGF-IR, significantly retarded growth of several cell lines *in vitro* [13], and retarded the growth of rhabdomyosarcoma xenografts [14]. Another IGF-1R-targeted antibody, SCH717454 was found to induce regressions in several sarcoma histotypes, notably osteosarcoma and Ewing sarcoma [15]. Characterization of the antibodies being developed suggests that there may be subtle differences in blocking binding of IGFs to the receptor (PH - unpublished data). Here we have evaluated the IMC-A12 antibody against the PPTP's *in vitro* panel of cell lines and its *in vivo* panels of solid tumor xenografts.

## MATERIALS AND METHODS

### *In vitro* testing

*In vitro* testing was performed using DIMSCAN, a semiautomatic fluorescence-based digital image microscopy system that quantifies viable cell numbers in tissue culture multiwell plates [16]. Cells were incubated in the presence of IMC-A12 for 96 hours at concentrations from 0.01 nM to 100 nM and analyzed as previously described [17].

### In vivo tumor growth inhibition studies

CB17SC-M *scid*$^{-/-}$ female mice (Taconic Farms, Germantown NY), were used to propagate subcutaneously implanted kidney/rhabdoid tumors, sarcomas (Ewing, osteosarcoma, rhabdomyosarcoma), neuroblastoma, and non-glioblastoma brain tumors, while BALB/c nu/nu mice were used for glioma models, as previously described [18-20]. All mice were maintained under barrier conditions and experiments were conducted using protocols and conditions approved by the institutional animal care and use committee of the appropriate consortium member. Tumor volumes ($cm^3$) were determined as previously described [21]. Responses were determined using three activity measures as previously described [21]. An

in-depth description of the analysis methods is included in the Supplemental Response Definitions section.

### Statistical Methods

The exact log-rank test, as implemented using Proc StatXact for SAS®, was used to compare event-free survival distributions between treatment and control groups. P-values were two-sided and were not adjusted for multiple comparisons given the exploratory nature of the studies.

### Drugs and Formulation

IMC-A12 was provided to the Pediatric Preclinical Testing Program by ImClone Systems through the Cancer Therapy Evaluation Program (NCI). IMC-A12 was administered intraperitoneally twice weekly for 6 weeks at a dose of 1 mg per animal. IMC-A12 was provided to each consortium investigator in coded vials for blinded testing.

## RESULTS

### IMC-A12 in vitro testing

IMC-A12 showed little evidence of treatment effect in the majority of the cell lines from the PPTP *in vitro* panel (Supplemental Table I). Three of 23 cell lines achieved at least 50% growth inhibition. These were the Ewing sarcoma cell lines, CHLA-9 and TC-71, and the rhabdomyosarcoma cell line, Rh41, which had $IC_{50}$ values of 49.31, 0.66 and 0.04 nM, respectively and which had $EC_{50}$ values of 0.03 nM or less (Supplemental Table 1).

### IMC-A12 in vivo testing

IMC-A12 was evaluated in 35 xenograft models. Fourteen of 690 mice died during the study (2.0%), with 6 of 344 in the control arms (1.7%) and 8 of 346 in the IMC-A12 treatment arms (2.3%). One line (BT-28) was excluded from analysis due to toxicity greater than 25 percent. A complete summary of results is provided in Supplemental Table II, including total numbers of mice, number of mice that died (or were otherwise excluded), numbers of mice with events and average times to event, tumor growth delay, as well as numbers of responses and T/C values.

Antitumor effects were evaluated using the PPTP activity measures for time to event (EFS T/C), tumor growth delay (tumor volume T/C), and objective response. IMC-A12 induced significant differences in EFS distributions compared to controls in 24/34 (71%) of solid tumor models (Table I). One line (Rh28) met the criteria for high activity with an EFS T/C value of >2.8 and with a final tumor volume less than the initial volume (Table I). An additional 13 of 33 evaluable solid tumor models met criteria for intermediate activity for the EFS T/C activity measure by having EFS T/C values exceeding 2.0 and significant differences in EFS distribution between treated and control groups. IMC-A12 was not tested against ALL xenograft models.

The *in vivo* testing results for the objective response measure of activity are presented in Figure 1 in a ‘heat-map’ format as well as a ‘COMPARE’-like format, based on the scoring criteria described in the Material and Methods and the Supplemental Response Definitions section. The latter analysis demonstrates relative tumor sensitivities around the midpoint score of 5 (stable disease). Objective responses were seen in one solid tumor model with a maintained complete response in the alveolar rhabdomyosarcoma line Rh28 (Figure 2). Figure 2 also illustrates three additional alveolar rhabdomyosarcoma xenografts (Rh10, Rh30, and Rh41), which demonstrated significant growth inhibition to IMC-A12 without achieving objective responses.

## DISCUSSION

IMC-A12 is a fully human IgG1 monoclonal antibody that binds with high affinity to IGF-IR, inhibiting ligand-dependent receptor activation and downstream signaling. IMC-A12 also mediates internalization and degradation of the IGF-IR [22]. IMC-A12 demonstrated relatively modest activity against the PPTP cell line panel where 50 percent growth inhibition was determined in only 3 (sarcoma) of 23 lines. As discussed previously [15], conditions of *in vitro* growth use high serum, which probably circumvents the effect of IGF-1R inhibition.

*In vivo*, IMC-A12, a species-specific antibody, demonstrated virtually no toxicity, but had broad-spectrum antitumor activity inducing significant differences in EFS distribution compared to control in 24 of 34 (71%) evaluable solid tumor xenografts. Significant differences in EFS distribution (treated to control) were observed in one or more xenografts for each histotype tested, with the exception of the medulloblastoma panel. IMC-A12 induced intermediate (n=13) or high (n=1) activity in 33 xenografts evaluable for this activity measure, including 6 of 6 rhabdomyosarcoma xenografts, 3 of 5 osteosarcoma xenografts, 2 of 5 neuroblastoma xenografts, and 1 of 5 Ewing sarcoma xenografts. The Wilms tumor panel and the medulloblastoma panel showed only low activity for the EFS T/C activity measure. The only objective response induced by IMC-A12 was observed in a rhabdomyosarcoma xenograft (Rh28) that achieved a maintained complete response. Two other alveolar rhabdomyosarcoma xenografts, Rh10, and Rh41 were also amongst the most sensitive to IMC-A12 treatment, consistent with the observation that the normally imprinted allele of the *IGF2* gene is activated in alveolar rhabdomyosarcoma [23]. PD2 (progressive disease with growth delay) responses were observed in an additional 16 xenografts.

Clinically, weekly doses of IMC-A12 ranging from 3 to 10 mg/kg have been well tolerated with no consistent adverse effects [22]. In adults, the plasma half-life values at the 3 and 6 mg/kg dose levels averaged 148 and 209 hours, while maximal IMC-A12 plasma concentrations were 333 and 415 μg/mL, respectively. Of importance to the current study, target trough concentrations of IMC-A12, as determined from preclinical studies in human tumor xenograft models, were achieved at the 6 mg/kg dose [22].

The PPTP previously evaluated another IGF-1R-targeted antibody [15]. Twenty-three *in vivo* models are common to both studies. Based on growth inhibition, similar activity for IMC-A12 and SCH717454 was observed in 13 models. Compared to the other antibody, IMC-A12 was superior in 5 models and inferior in 5 models. While the overall patterns of response were similar, there were differences. For example, IMC-A12 had greater activity against 3 of 5 rhabdomyosarcoma xenografts, but less activity in 2 of 4 Ewing sarcomas and 2 of 5 osteosarcoma xenografts. Of interest is that rhabdomyosarcomas are predominantly IGF-2-driven whereas Ewing sarcomas and many osteosarcomas primarily secrete IGF-1. Reference to the PPTP Affymetrix expression profiles (pptp.stjude.org/affyData.php) showed that 4/5 Ewing sarcoma xenografts had high expression of IGF-1 ligand, whereas all 8 rhabdomyosarcomas and 7/8 neuroblastomas had high level expression of IGF-2 ligand. The osteosarcoma models were evenly divided into those with high IGF-1 or high IGF-2 expression. IGF-2 expression was strong in 5/14 brain tumors, but only a single line (BT-41) expressed IGF-1. Only 3/10 ALL xenografts expressed IGF-2 ligand, and none expressed IGF-1 signal. Thus, there is no apparent correlation between expression of ligand and tumor sensitivity to IMC-A12.

Several strategies for inhibiting IGF-1R-mediated signaling are in clinical or preclinical development. These include small molecule inhibitors of IGF-1R, receptor-binding antibodies such as IMC-A12, and antibodies that directly bind ligands. Results presented

here, and previously [15] indicate that the predominant effect of antibodies that block ligand binding to IGF-1R is to slow tumor progression, rather than induce a high frequency of tumor regressions. IGF's act as survival factors for numerous cellular stresses, including cytotoxic agents used in treatment of childhood cancer. Consequently, for pediatric cancer one rational use of agents such as IMC-A12 is to combine these agents with current curative chemotherapy. A second approach will be to evaluate IMC-A12 in combination with other signaling inhibitors, such as rapamycin (sirolimus), against the PPTP *in vivo panel*. Combinations of IMC-A12 with standard chemotherapy agents and with molecularly targeted agents (e.g., cetuximab, erlotinib, temsirolimus) are being studied in clinical trials for adults with cancer and pediatric evaluations of IMC-A12 have been initiated.

## Supplementary Material

Refer to Web version on PubMed Central for supplementary material.

## Acknowledgments

This work was supported by NO1-CM-42216, CA21765, and CA108786 from the National Cancer Institute and used IMC-A12 supplied by ImClone Systems. In addition to the authors represents work contributed by the following: Sherry Ansher, Catherine A. Billups, Joshua Courtright, Edward Favours, Henry S. Friedman, Debbie Payne-Turner, Charles Stopford, Chandra Tucker, Amy E. Watkins, Joe Zeidner, Ellen Zhang, and Jian Zhang.

## Reference List

1. Minniti CP, Tsokos M, Newton WA Jr. et al. Specific expression of insulin-like growth factor-II in rhabdomyosarcoma tumor cells. Am J Clin Pathol. 1994; 101(2):198–203. [PubMed: 8116575]
2. Sepp-Lorenzino L. Structure and function of the insulin-like growth factor I receptor. Breast Cancer Res Treat. 1998; 47(3):235–253. [PubMed: 9516079]
3. Stewart CE, Rotwein P. Growth, differentiation, and survival: multiple physiological functions for insulin-like growth factors. Physiol Rev. 1996; 76(4):1005–1026. [PubMed: 8874492]
4. Kaleko M, Rutter WJ, Miller AD. Overexpression of the human insulinlike growth factor I receptor promotes ligand-dependent neoplastic transformation. Mol Cell Biol. 1990; 10(2):464–473. [PubMed: 2153917]
5. LeRoith D, Baserga R, Helman L, et al. Insulin-like growth factors and cancer. Ann Intern Med. 1995; 122(1):54–59. [PubMed: 7619109]
6. Kurmasheva RT, Houghton PJ. IGF-I mediated survival pathways in normal and malignant cells. Biochim Biophys Acta. 2006; 1766(1):1–22. [PubMed: 16844299]
7. Braczkowski R, Schally AV, Plonowski A, et al. Inhibition of proliferation in human MNNG/HOS osteosarcoma and SK-ES-1 Ewing sarcoma cell lines in vitro and in vivo by antagonists of growth hormone-releasing hormone: effects on insulin-like growth factor II. Cancer. 2002; 95(8):1735–1745. [PubMed: 12365022]
8. Cohen BD, Baker DA, Soderstrom C, et al. Combination therapy enhances the inhibition of tumor growth with the fully human anti-type 1 insulin-like growth factor receptor monoclonal antibody CP-751,871. Clin Cancer Res. 2005; 11(5):2063–2073. [PubMed: 15756033]
9. Wang Y, Hailey J, Williams D, et al. Inhibition of insulin-like growth factor-I receptor (IGF-IR) signaling and tumor cell growth by a fully human neutralizing anti-IGF-IR antibody. Mol Cancer Ther. 2005; 4(8):1214–1221. [PubMed: 16093437]
10. Sachdev D, Yee D. Inhibitors of insulin-like growth factor signaling: a therapeutic approach for breast cancer. J Mammary Gland Biol Neoplasia. 2006; 11(1):27–39. [PubMed: 16947084]
11. Sachdev D, Yee D. Disrupting insulin-like growth factor signaling as a potential cancer therapy. Mol Cancer Ther. 2007; 6(1):1–12. [PubMed: 17237261]
12. Guerreiro AS, Boller D, Doepfner KT, et al. IGF-IR: potential role in antitumor agents. Drug News Perspect. 2006; 19(5):261–272. [PubMed: 16941048]

13. El-Badry OM, Minniti C, Kohn EC, et al. Insulin-like growth factor II acts as an autocrine growth and motility factor in human rhabdomyosarcoma tumors. Cell Growth Differ. 1990; 1(7):325–331. [PubMed: 2177632]

14. Kalebic T, Tsokos M, Helman LJ. In vivo treatment with antibody against IGF-1 receptor suppresses growth of human rhabdomyosarcoma and down-regulates p34cdc2. Cancer Res. 1994; 54(21):5531–5534. [PubMed: 7923191]

15. Kolb EA, Gorlick R, Houghton PJ, et al. Initial testing (stage 1) of a monoclonal antibody (SCH 717454) against the IGF-1 receptor by the pediatric preclinical testing program. Pediatr Blood Cancer. 2008; 50(6):1190–1197. [PubMed: 18260118]

16. Frgala T, Kalous O, Proffitt RT, et al. A fluorescence microplate cytotoxicity assay with a 4-log dynamic range that identifies synergistic drug combinations. Mol Cancer Ther. 2007; 6(3):886–897. [PubMed: 17363483]

17. Houghton PJ, Morton CL, Kolb EA, et al. Initial testing (stage 1) of the proteasome inhibitor bortezomib by the pediatric preclinical testing program. Pediatr Blood Cancer. 2008; 50(1):37–45. [PubMed: 17420992]

18. Friedman HS, Colvin OM, Skapek SX, et al. Experimental chemotherapy of human medulloblastoma cell lines and transplantable xenografts with bifunctional alkylating agents. Cancer Res. 1988; 48(15):4189–4195. [PubMed: 3390813]

19. Graham C, Tucker C, Creech J, et al. Evaluation of the antitumor efficacy, pharmacokinetics, and pharmacodynamics of the histone deacetylase inhibitor depsipeptide in childhood cancer models in vivo. Clin Cancer Res. 2006; 12(1):223–234. [PubMed: 16397046]

20. Peterson JK, Tucker C, Favours E, et al. In vivo evaluation of ixabepilone (BMS247550), a novel epothilone B derivative, against pediatric cancer models. Clin Cancer Res. 2005; 11(19 Pt 1): 6950–6958. [PubMed: 16203787]

21. Houghton PJ, Morton CL, Tucker C, et al. The pediatric preclinical testing program: description of models and early testing results. Pediatr Blood Cancer. 2007; 49(7):928–940. [PubMed: 17066459]

22. Rowinsky EK, Youssoufian H, Tonra JR, et al. IMC-A12, a human IgG1 monoclonal antibody to the insulin-like growth factor I receptor. Clin Cancer Res. 2007; 13(18 Pt 2):5549s–5555s. [PubMed: 17875788]

23. Zhan S, Shapiro DN, Helman LJ. Activation of an imprinted allele of the insulin-like growth factor II gene implicated in rhabdomyosarcoma. J Clin Invest. 1994; 94(1):445–448. [PubMed: 8040287]

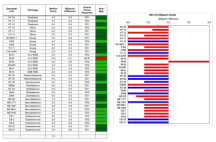

**Figure 1.**

IMC-A12 *in vivo* objective response activity. Left: The colored ‘heat map’ depicts group response scores. A high level of activity is indicated by a score of 6 or more, intermediate activity by a score of ≥ 2 but < 6, and low activity by a score of < 2. Right: representation of tumor sensitivity based on the difference of individual tumor lines from the midpoint response (stable disease). Bars to the right of the median represent lines that are more sensitive, and to the left are tumor models that are less sensitive. Red bars indicate lines with a significant difference in EFS distribution between treatment and control groups, while blue bars indicate lines for which the EFS distributions were not significantly different.

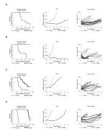

**Figure 2.**
IMC-A12 activity against individual solid tumor xenografts. Kaplan-Meier curves for EFS, median relative tumor volume graphs, and individual tumor volume graphs are shown for selected lines: (A) Rh10, (B) Rh28, (C) Rh30 and (D) Rh41.

**Table I**

Activity for IMC-A12 against the PPTP *in Vivo* Panel

| Xenograft Line | Histology | KM Estimate of Median Time to Event | P-value | EFS T/C | Median Final RTV | Tumor Volume T/C | P-value | T/C Activity | EFS Activity | Response Activity |
|---|---|---|---|---|---|---|---|---|---|---|
| BT-29 | Rhabdoid | 30.9 | <0.001 | 1.4 | >4 | 0.66 | 0.023 | Low | Low | Low |
| KT-14 | Rhabdoid | > EP | <0.001 | > 2.3 | 1.4 | 0.34 | <0.001 | Int | Int | Int |
| KT-12 | Rhabdoid | 10.9 | 0.034 | 1.2 | >4 | 0.81 | 0.165 | Low | Low | Low |
| KT-10 | Wilms | 10.8 | 0.006 | 1.6 | >4 | 0.63 | 0.007 | Low | Low | Int |
| KT-11 | Wilms | 14.7 | 0.006 | 1.4 | >4 | 0.66 | 0.029 | Low | Low | Low |
| KT-13 | Wilms | 11.4 | 0.282 | 1.3 | >4 | 0.74 | 0.436 | Low | Low | Low |
| SK-NEP-1 | Ewing | 10.2 | 0.043 | 1.2 | >4 | 0.69 | 0.063 | Low | Low | Low |
| EW5 | Ewing | 17.6 | <0.001 | 2.6 | >4 | 0.39 | <0.001 | Int | Int | Int |
| EW8 | Ewing | 14.7 | 0.032 | 1.2 | >4 | 0.62 | 0.004 | Low | Low | Low |
| TC-71 | Ewing | 9 | 0.698 | 1 | >4 | 0.88 | 0.393 | Low | Low | Low |
| CHLA258 | Ewing | 13.1 | 0.03 | 1.3 | >4 | 0.67 | 0.052 | Low | Low | Low |
| Rh10 | ALV RMS | > EP | <0.001 | > 2.1 | 1.9 | 0.24 | <0.001 | Int | Int | Int |
| Rh28 | ALV RMS | > EP | <0.001 | > 2.8 | 0 | 0.15 | <0.001 | Int | High | High |
| Rh30 | ALV RMS | 30.5 | 0.004 | 2.3 | >4 | 0.41 | 0.007 | Int | Int | Int |
| Rh30R | ALV RMS | 31.8 | <0.001 | 2.4 | >4 | 0.44 | <0.001 | Int | Int | Int |
| Rh41 | ALV RMS | 38.6 | <0.001 | 3.3 | >4 | 0.17 | <0.001 | Int | Int | Int |
| Rh18 | EMB RMS | 26.5 | <0.001 | 3 | >4 | 0.33 | <0.001 | Int | Int | Int |
| BT-45 | Medulloblastoma | 7.1 | 0.612 | 1.1 | >4 | 0.81 | 0.739 | Low | Low | Low |
| BT-50 | Medulloblastoma | 35.7 | 0.643 | 1 | >4 | 1.04 | 0.684 | Low | Low | Low |
| BT-36 | Ependymoma | > EP | 1 | . | 1.8 | 0.89 | 0.853 | Low | NE | Int |
| GBM2 | Glioblastoma | 21.7 | <0.001 | 1.4 | >4 | 0.33 | <0.001 | Int | Low | Low |
| BT-39 | Glioblastoma | 17.1 | 0.355 | 1.2 | >4 | 0.84 | 0.529 | Low | Low | Low |

| Xenograft Line | Histology | KM Estimate of Median Time to Event | P-value | EFS T/C | Median Final RTV | Tumor Volume T/C | P-value | T/C Activity | EFS Activity | Response Activity |
|---|---|---|---|---|---|---|---|---|---|---|
| D645 | Glioblastoma | 17.2 | <0.001 | 2.3 | >4 | 0.44 | <0.001 | Int | Int | Int |
| D456 | Glioblastoma | 9.7 | 0.304 | 1.1 | >4 | 0.87 | 0.28 | Low | Low | Low |
| NB-SD | Neuroblastoma | 9.9 | 0.013 | 1.6 | >4 | 0.58 | 0.021 | Low | Low | Low |
| NB-1771 | Neuroblastoma | 13.1 | <0.001 | 3.6 | >4 | 0.12 | <0.001 | High | Int | Int |
| NB-1691 | Neuroblastoma | 12.3 | 0.268 | 1.4 | >4 | 0.79 | 0.387 | Low | Low | Low |
| NB-EBc1 | Neuroblastoma | 11 | 0.041 | 2 | >4 | 0.42 | 0.01 | Int | Low | Int |
| NB-1643 | Neuroblastoma | 26.3 | <0.001 | 4.2 | >4 | 0.35 | <0.001 | Int | Int | Int |
| OS-1 | Osteosarcoma | > EP | <0.001 | > 2.3 | 3.4 | 0.47 | <0.001 | Low | Int | Int |
| OS-2 | Osteosarcoma | 34.2 | <0.001 | 2.1 | >4 | 0.38 | <0.001 | Int | Int | Int |
| OS-9 | Osteosarcoma | > EP | <0.001 | > 2.3 | 3.1 | 0.41 | <0.001 | Int | Int | Int |
| OS-33 | Osteosarcoma | 11.6 | 0.323 | 0.9 | >4 | 1.02 | 0.481 | Low | Low | Low |
| OS-31 | Osteosarcoma | 20.3 | 0.367 | 1 | >4 | 0.92 | 0.393 | Low | Low | Low |